Flow Measurement and Instrumentation 96 (2024) 102557

Contents lists available at ScienceDirect

Flow Measurement and Instrumentation

journal homepage: www.elsevier.com/locate/flowmeasinst

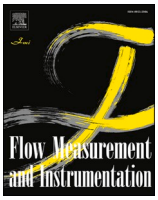

Natural surface floaters in image-based river surface velocimetry: Insights from a case study

Hang Trieu [a,*], Per Bergström [a], Mikael Sjödahl [a], J.Gunnar I. Hellström [a], Patrik Andreasson [b,c], Henrik Lycksam [a]

[a] Division of Fluid and Experimental Mechanics, Luleå University of Technology, 97754, Luleå, Sweden
[b] Vattenfall AB, Research & Development (R & D), Hydraulic Laboratory, 81426, Älvkarleby, Sweden
[c] Wildlife, Fish and Environmental Studies, Swedish University of Agricultural Sciences, 901 83, Umeå, Sweden

ARTICLE INFO

Keywords:
Image velocimetry
Photogrammetry
3D-LPTV
Surface flow velocity
Image tracking

ABSTRACT

This study focuses on utilizing image techniques for river velocity measurement, with a specific emphasis on natural surface floating patterns. Employing a multi-camera system, we conducted 3D measurements on river surfaces, including surface velocity and water surface reconstruction. A pattern-based tracking approach has been adopted to improve the performance of image measurements on different types of natural floating tracers. The study employs the following approaches: 3D Lagrangian Pattern Tracking Velocimetry (3D-LPTV), 2D Lagrangian Pattern Velocimetry (2D- LPTV), and Large-scale Particle Image Velocimetry (LSPIV), for surface velocity estimation. The outcomes revealed that all three approaches yielded consistent results in terms of averaged velocity. However, the LSPIV method produced about two times higher uncertainty in measured velocities compared to the other methods. A strategy to assess the quality of river surface patterns in velocity estimation is presented. Specifically, the sum of squared interrogation area intensity gradient (SSIAIG) was found to be strongly correlated with measurement uncertainty. Additionally, a term related to the peak sidelobe ratio (PSR) of the cross-correlation map was found as an effective constraint, ensuring the image-tracking process achieves high reliability. The precision of measurements increases corresponding to the increase of image intensity gradient and PSR.

1. Introduction

River velocimetry holds significance in various hydraulic and hydrological applications. Understanding river flow aids environmental assessments including estimating flow discharge and assessing aquatic environments such as fish passage and habitats, pollutant and river erosion, and debris transport [1–4]. It also contributes to monitoring water quality and managing water resources [5–7]. River velocity is an important metric in hydraulic engineering applications for constructing structures such as bridges, dams, and channels to ensure their stability and endurance [8]. The capacity to accurately estimate the stream velocity is important in flood prediction and management, protecting communities and infrastructure [9,10].

Hydropower is the largest source of renewable energy production in Sweden, accounting for approximately 45% of Swedish electricity generation [11]. Flow velocity measurements in the vicinity of hydropower facilities are critical in a variety of practical applications to ensure sustainable hydropower and develop hydropower production. Measuring these streams, however, imposes challenges due to their vast and complicated geometry. This work aims to adapt non-intrusive surface velocity measurements in natural streams and to increase the ability to use naturally occurring surface patterns in rivers as tracers.

In most open channels, flow velocity is usually conducted directly by contact devices such as acoustic Doppler velocimetry (ADV), current meters, or velocity propellers. These methods are expensive and time-consuming to perform, and the measurement process requires contact with the water body. To limit safety hazards for operators and equipment, these surveys are normally performed during low or moderate flow conditions. A more advanced technique, the acquisition of flow velocity and depth can be conducted simultaneously with acoustic Doppler current profilers (ADCPs) [12,13]. Measurements can be executed along transects of wide rivers with small boats, however the sensor is expensive and must be in contact with the waterbody thus limiting its use in more intense flow conditions.

* Corresponding author.
E-mail address: hang.trieu@ltu.se (H. Trieu).

https://doi.org/10.1016/j.flowmeasinst.2024.102557
Received 29 September 2023; Received in revised form 8 January 2024; Accepted 8 February 2024
Available online 13 February 2024

In contrast to contact methods, noncontact flow estimation approaches such as radar [14] and thermal infrared imaging [15] show several advantages due to their relaxation from flow disturbance and damage. However these options rarely reduce the issues related to costs and are time-consuming.

Traditional river velocity measurement devices, both contact and noncontact are typically expensive and provide limited spatial coverage. In laboratory hydraulic experiments, image-based velocimetry such as Particle Image Velocimetry (PIV) and Particle Tracking Velocimetry (PTV) are widely employed and have been standard techniques over the last three decades [16–18]. PIV takes an Eulerian perspective by calculating shifts in distinctive intensity patterns of groups of tracer particles in small interrogation areas (IA) across at least two frames with a known time lag and analyzing instantaneous velocity. In contrast, PTV adopts a Lagrangian point of view that determines the velocity and reconstructs the path of the individual particles. Both PIV and PTV techniques were originally developed for laboratory experiments and essentially extend the basic principles to the large-scale situations known as Large-scale Particle Velocimetry (LSPIV) [8] and Large-scale Particle Tracking Velocimetry (LSPTV). Furthermore, there are other alternative image-based velocimetry techniques, for instance, Space-Time Image velocimetry (Fujita et al., 2015; [19]) and optical flow applications [20,21]. With affordable and flexible image systems available in recent years, these approaches have advanced our ability to perform noninvasive natural flow observations at a high temporal resolution to help overcome the limitations of traditional measurement methods.

In river surface velocity measurements, flow seeding is an unavoidable task in some situations where the water flow is clear and there is no occurrence of floating materials on the surface. Surface seeding should involve the use of non-polluting and non-harmful materials. It is advisable to choose non-toxic and biodegradable seeding materials. Additionally, depending on the goal of the adopted methods, for instance, LSPIV or PTV, the surface seeding material will be chosen based on the shape and size as well as the ability to travel on the flow surface. While LSPIV requires particles to be densely and homogeneously distributed, PTV approaches need sparse and highly defined shaped particles. The seeding task in actual field conditions may face some challenges when the measurement tends to observe a large area of water. Moreover, the seeding quality is not always ensured due to human and outdoor environments such as wind and river reach characteristics. Investigations on optimizing tracer seeding for image-based velocimetry, Dal Sasso et al. [22], Dal Sasso et al. [23], Dal Sasso et al. [24] and Pizarro et al. [25], Pizarro et al. [25] revealed that spatial distribution and seeding characteristics have a significant impact on the performances of surface velocity measurement in rivers. To improve LSPIV results in low-density seeding conditions, Strelnikova et al. [26] investigate ensemble correlation method in processing relatively short image sequences. The ensemble method involves averaging the correlation matrices across the entire image sequence before searching for the correlation peak. Their finding was that this technique yields a more well-defined correlation peak, particularly in low-density seeding conditions, resulting in improved LSPIV results. Ensemble correlation would most likely improve the results in stationary flow conditions; however it is outside the scope of this investigation and therefore left for future improvement.

A measurement station setup with low-cost digital image storage was used to monitor the streamflow regime over long time spans [27]; the study demonstrates that PTV continuously can yield reliable surface-flow velocity estimates. For such applications, the ability to use the presence of natural floating patterns on the flow surface would increase the insight into the various flow conditions in real-time. In clear water flow, when floaters may individually travel through the field of view, the PTV approach would be appropriate to deploy. However, for PTV shape of the surface particle needs to be clearly defined. For example, Tauro et al. [28] successfully estimated the surface velocity of streamflow using PTV-stream with artificial seeding particles. The same tool was applied to measure a moderate flood at a river, the outcome of the study demonstrated the potential of the tool but also raised challenges in using floating debris as particles for traditional PTV. In high turbulence flow where turbulent structures are evident on the surface, the water flow itself provides a continuously floating pattern in images which can be used as a flow pattern for velocity estimation. Hence, for such flow conditions the LSPIV approach is more suitable. For example, Dramais et al. [29] investigated a mobile LSPIV system for remote stream gauging, employing it to measure velocity during a flushing event, wherein the turbulent flow itself was utilized in LSPIV.

In most LSPIV studies, the flow surface is assumed as an inclined or horizontal plane when performing surface velocity measurements in rivers. Cameras are required to face in nadir angle to the water surface [30] or image frames have to be orthorectified to counteract the considerable distortions caused by the camera's viewing angle ([31]; Fujita et al., 2015; [32]). The assumption of a 2D plane water surface may be acceptable for low to moderate flow conditions with regular riverbeds but not for steep rivers and extreme free-surface deformation in high-flow situations. Thus, multiple cameras are required to avoid making any necessary assumptions about the surface or image orthorectification. This method enables the estimation of 3D water surface as well as water level variation. For example, Li et al. [33] utilized a stereo-imaging system to estimate the surface velocity field and water surface distribution of a mountainous stream. Therein, the influence of uneven surface on LSPIV measurements is demonstrated by significant disparities between a 3D reconstructed water surface, inclined planar surface, and horizontal plane assumptions.

Given the challenges arising from non-ideal surface particles in river velocimetry, particularly in measuring extensive areas where seeding also presents an issue, we aim to optimize the ability to use natural floating surface patterns rather than artificial seeding particles in circumstances where surface floaters exist. To estimate the 3D magnitude of velocity and the 3D elevation of the river surface, a three-camera imaging system is employed to capture natural surface patterns passing through the field of view. Because the surface floating patterns are intermittent in the field of view, the Lagrangian Particle Tracking technique is used to track the floaters in image sequences. However, the movement of the flow surface is assessed using surface patterns represented by sub-regions made up of groups of floating material rather than singularly specific particles. Positions of surface points are defined using a camera network correlation approach to preserve good regions of interest for tracking and discard unqualified surface regions. Similar to the traditional PIV interrogation method, sub-image searching is determined using image cross-correlation. The instantaneous surface velocity field between successive frames is computed, and trajectories for the whole image sequence are reconstructed by the triangulation process from calibrated cameras.

In this paper, the river surface velocimetry based on the Lagrangian approach is named Lagrangian Pattern Tracking Velocimetry (LPTV). We present a multiple-camera system that enables the estimation of 3D surface velocity magnitude and the reconstruction of 3D river surface, using natural floaters on the river surface that pass through the field of view. A series of field measurements were conducted in a river utilizing various natural surface floating patterns. To demonstrate the solution, a comparison of sub-image-based 3D-LPTV, 2D-LPTV and 2D- LSPIV is presented. An outlier filtering strategy based on image matching and post-processing is described. Given the lack of benchmark velocity in these measurements, the goal of this work is not to investigate the impact of different surface patterns on these three approaches. Instead, the main objective of this study is to examine the suitability of natural surface floaters in river velocimetry through a set of typical river surface patterns observed in a case study. Two parameters are employed in describing the characteristics of river surface patterns: these parameters are derived from calculations based on the image intensity gradient and the strength of cross-correlation maps in the pattern tracking process.

The paper is structured as follows: The descriptions of the measurement system and field measurement are introduced in Section 2; Section 3 describes the approaches for surface velocity observation; The image processing procedure is presented in Section 4; Results of velocity measurement, analyses on characteristics of river surface patterns and discussion are presented in Section 5; Section 6 discusses factors to consider when conducting image-based river velocimetry in natural streams; Concluding remarks are summarized in Section 7.

2. Measurement setting

This section provides comprehensive information about the measurement site and the imaging system employed for the measurements. It includes details about the field conditions and the characteristic variations of the river floating patterns captured in these measurements.

2.1. Measurement site and imaging system configuration

Experiments were carried out in Luleå river at Boden, Sweden (Svedjebron bridge 75°12′45.814″ Latitude, 395°9′22.5″ in WGS 84 coordinate system) on the 24th May and the June 4, 2021. The flow discharges during the experiments were in the range of 809–894 m^3/s on the 24th May and 663–730 m^3/s on the 4th of June, respectively, according to data collected by the Boden hydropower plant about 800 m upstream of the measurement position. The camera system consists of three cameras (Genie-Nano-5G) with a resolution of 2464 × 2056 pixels and are equipped with 16 mm objective lens. The images can be captured synchronously by the cameras mounted on the bridge at varying frame rates, with a maximum of 80 frames per second (fps). The setup had a field of view of 7 × 6 m^2 on the river surface and had a ground sampling distance roughly of 0.23 cm/pixel. The measurements were carried out in the late spring when the flow through the upstream Boden hydroelectric facility was relatively high, and spillway was open. A sketch of the measurement setup is presented in Fig. 1.

The measurements were performed in daytime sunshine conditions. Camera calibration to establish the interior and exterior camera parameters was done at the measurement site to assure the reliability of camera parameters. The camera calibration technique is detailed in Trieu et al. [34].

2.2. River surface floating tracers

In situations where natural tracer particles are not present, artificial seeding is required to improve the reliability of measurements [34]. However, providing sufficient seeding that covers a large water surface area can be challenging, particularly when the field of view is large, and the seeding position is too far from the water surface. In cases where natural surface floaters are present, surface velocity analysis can be performed without requiring artificial flow seeding. However, natural surface floaters are usually randomly and discontinuously distributed, and they come in various shapes and sizes. Both natural and artificial seeding usually rapidly changes from being evenly distributed to being clustered into meandering flow structures due to secondary currents that always are present in rivers. Fig. 2 shows reference examples of the natural surface floaters observed throughout the measurement campaign, offering a better understanding of their variations in distribution, shapes, and sizes. To evaluate the utilization of these surface floating patterns, it is crucial to have a thorough understanding of the characteristics that influence the performance of image-based velocimetry. Pattern C presents itself as a cloudy foam layer in the river, whereas Pattern B is composed of smaller and more dispersed surface floaters. In contrast, Pattern A exhibits even smaller and more evenly distributed surface floaters.

3. Image-based approaches for river surface velocimetry: LPTV and LSPIV

PIV and PTV are based on Eulerian and Lagrangian frames of reference (i.e., algorithms, point of view). Each algorithm has its own set of assumptions and constraints. For instance, for reliable results, the Eulerian approach requires a steady state of flow and a consistent quantity of tracers present throughout the processing time, conversely, the Lagrangian approach is less concerned with flow steadiness because it specifies the particle's position at any given time but is however difficult to characterize when tracers are dense and regularly interact with one another [35]. The grayscale distribution characteristics such as image contrast and feature size of naturally occurring surface floaters (as illustrated in Fig. 2), exhibit inhomogeneity in space and discontinuity in time. As a result, the PIV approach may be adversely affected since it calculates the average velocity by analyzing velocities across fixed space points on the river surface throughout the entire image sequence. Furthermore, due to the non-uniform and ill-defined shapes of the river surface floaters, the conventional PTV approach is similarly unsuitable for this type of particle. The surface materials under consideration resemble patterns rather than single particles.

The present study utilizes a pattern-based Lagrangian approach, in which surface patterns representing interrogation areas or sub-images are tracked throughout the entire sequence of images. This method utilizes naturally occurring surface floating patterns that are intermittent in the river. Consequently, LPTV is employed to reconstruct the flow

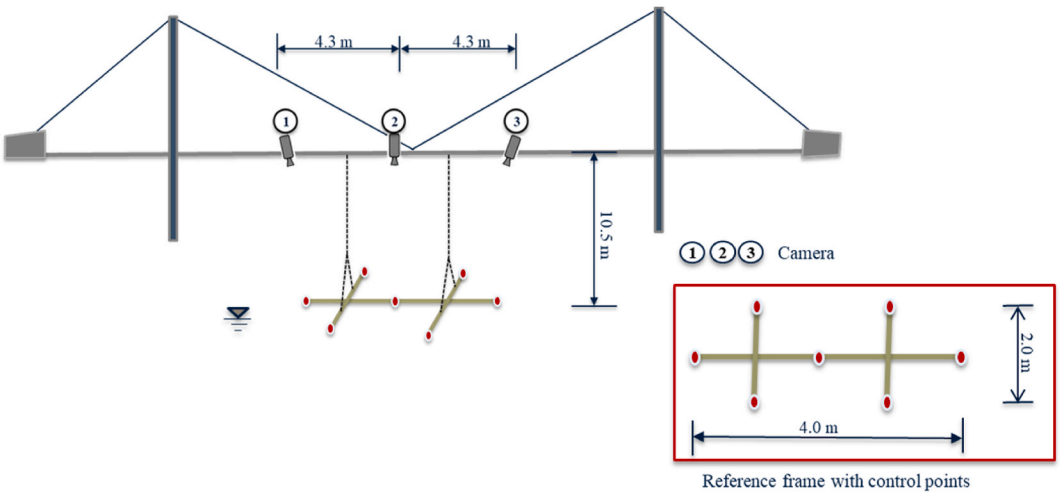

Fig. 1. Sketch of river surface velocimetry setup.

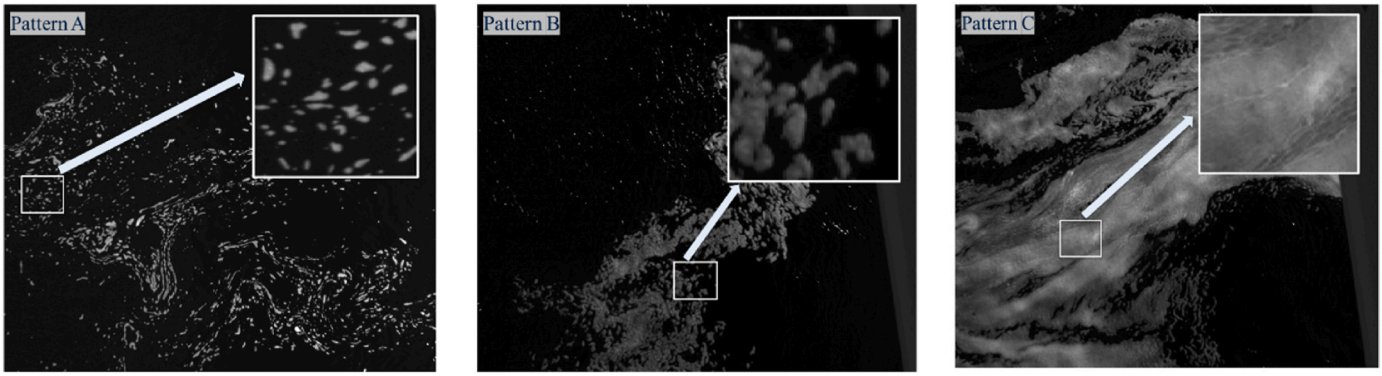

Fig. 2. River surface patterns in different measurements: original images.

paths of individual sub-images.

4. Image processing procedure

This section provides a detailed description of two primary techniques employed for image processing and analysis. Fig. 3 illustrates a flowchart that outlines the image processing and analysis. The first technique (3D-LPTV) involves the determination of surface velocity in a 3D coordinates system utilizing all the cameras within the imaging setup. In this regard, the coordinates of the surface points are obtained through optical triangulation. The second technique (2D-LPTV, LSPIV) involves image-based velocimetry using a single camera. In this approach, the images need to be undistorted and orthorectified utilizing a projective transformation based on Ground Control Points (GCPs). The latter method manipulates the image such that all pixels have the same spatial length. It should be noted that no pre-processing has been applied to the frame in 3D-LPTV to ensure a consistent comparison of the performance of various river surface floaters observed in this study (see

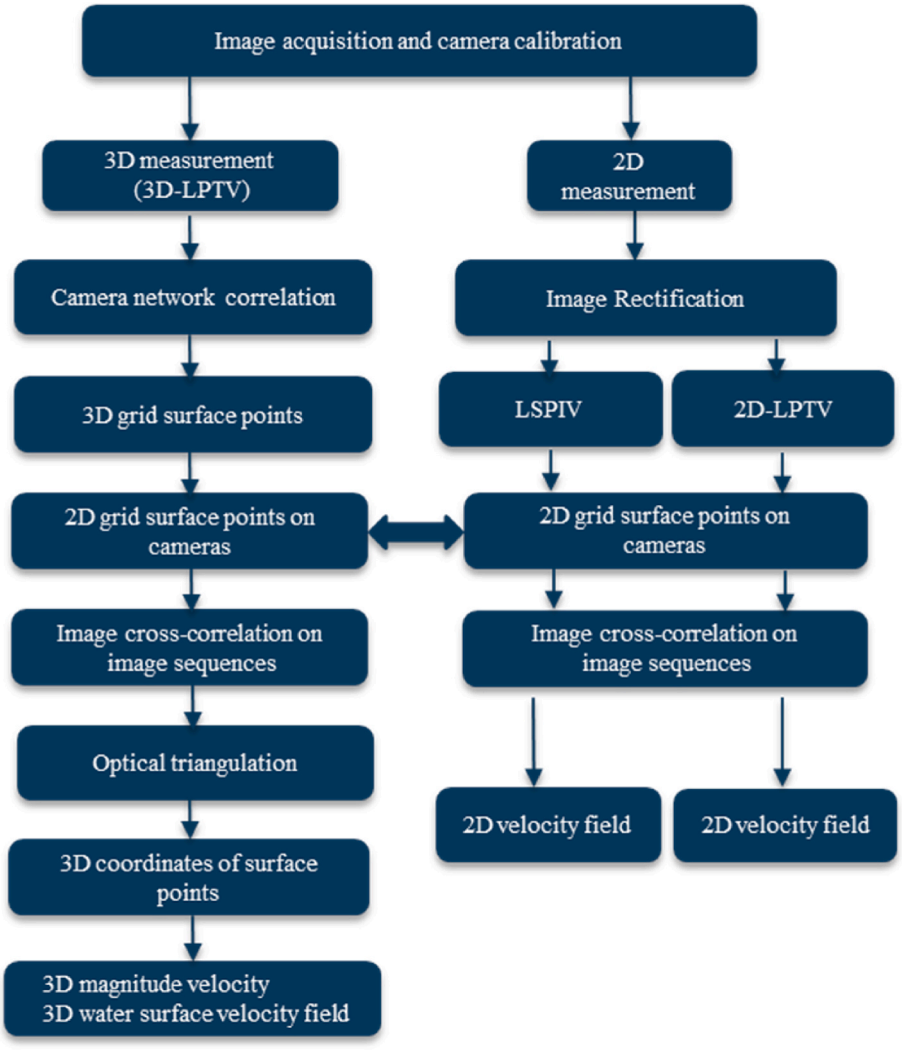

Fig. 3. Flow chart of image processing and analysis.

Section 5.3). The following subsections elaborate on the specific aspects of velocity estimation using a multi-camera system and a single camera, respectively.

4.1. Image pre-processing

Pre-processing is a main stage in the methodology in the image-based river surface velocimetry. It involves rectifying lens distortions, orthorectifying images, and stabilizing them if necessary. Additionally, various filters or adjustments may also be applied to enhance the visibility and clarity of seeding particles [36]. In this study, orthorectification was applied only to the images in 2D-LPTV and LSPIV to correct perspective distortion and standardize pixel dimensions. No pre-processing procedures were employed in 3D-LPTV. Literature often involves pre-processing river flow data to improve surface features [24,26,37]. Common techniques typically include contrast enhancement, noise reduction using filters, and background subtraction. This study focuses on examining the grayscale distribution characteristics of various observed river surface features. Enhancement techniques therefore were not utilized on images, allowing for a raw comparison of the different surface patterns in the velocity estimation, as they are beyond the scope of this study.

In LSPIV and LSPTV, the interrogation area size should be large enough to encompass a sufficient particle density for cross-correlation but small enough to avoid ambiguous outcomes [37,38]. Recent work by Ref. [36] highlighted the significant impact of frame rate on image velocimetry results, particularly concerning the LSPIV technique. This study aims to analyze the influence of surface floating patterns on image velocimetry. The analysis focuses on assessing the sensitivity of measured velocities concerning the changes in image intensity gradient and the strength of cross-correlation maps between consecutive frames. To maintain consistency, all other parameters remain constant, including the sampling frequency of 24.3 fps, 20 frames for each dataset, and the utilization of the same IA across all datasets.

4.2. Camera network correlation and definition of river surface points

To be able to determine river surface points in a spatial coordinate system, the initial step involves identifying homologous points across all cameras. These homologous points correspond to image points representing the same locations on the river surface. Camera network correlation aims to find the homologous points representing the spatial grid surface points within the measured area. Initially, these grid surface points are approximated under the assumption of a planar water surface. The camera network correlation starts with the initial approximated coordinate of a 3D surface point. Subsequently, adjustments are made to refine its coordinates, aiming to determine its optimal position. This adjustment facilitates achieving the best possible cross-correlation across all camera pairs upon reprojecting the point onto the cameras. The camera network correlation procedure for each grid point follows this sequence:

The approximated 3D surface point is assumed to be at a distance d from its estimated planar position in the normal direction. The correlation between camera pairs is performed for each incremental or ray tracing step of $[-d, d]$, to find $\Delta d_{\max}$, which corresponds to the maximum of the camera pair's correlation coefficient. To be more specific, each incremental 3D surface point is reprojected onto the images of each camera in the network to get corresponding image points. Sub-images for cross-correlation are generated from these image points. Cross-correlation method is used as a measure to define the similarity between corresponding sub-images in image pairs. In the three-camera system correlation is performed for all three camera pairs. The median position of the correlation peaks is considered as the detected surface point in the system. The incremental step that corresponds to the correlation peak is selected as the optimal point within the range of $[-d,d]$, providing the highest correlation for the camera network. This best incremental point is then used to recalculate the 3D coordinates of the surface point from its initial approximated position. Fig. 4a and b show examples of the correlation between the three camera pairs in the network for grid surface points 88 and 89, respectively. The best-adjusted 3D points on the water surface are reprojected onto the images of each camera in the network. As a result, grid surface points on the image are determined (see Fig. 4c). The correlation results from the camera network are used as filtering criteria in the image processing procedure (see Section 4.4). In this case, the correlation for point 88 yields a median value of 0.5, and for point 89, a median value of 0.99 (see Fig. 4a and b). Consequently, grid surface point 88 is labeled as invalid, while point 89 is marked as a valid surface point for the measurement. Fig. 4c shows only valid surface points after applying filtering criterion in the camera network correlation stage. This filtering criterion serves to retain good regions for image tracking while excluding surface regions that do not meet the required criteria from the calculation (Fig. 4c).

4.3. Calibrated image orthorectification and 2D velocity measurement

In LSPIV application, orthorectification needs to be carried out to correct images from perspective distortion. To orthorectify an image, imaged GCPs with known real-world coordinates are established in the field of view and paired with their pixel locations. Using the camera calibration, we calculate the spatial coordinates of points on the water surface. A set of points on the river surface is therefore used as GCPs, assuming the water surface of the analyzed area of interest represents a plane. A 2D transformation that represents 8 parameters of perspective projection between the spatial coordinates and projection of these GCPs onto the image [32,39]. The image orthorectification was carried out using MATLAB 2019b to generate the orthorectified images utilized in this analysis.

Fig. 5 shows an example of the original image and orthorectified image as well as corresponding water surface points in these two images. 2D velocity estimations (i.e., PTV and LSPIV) are performed on rectified images. As a result, the 2D velocity magnitudes of the instantaneous and average surface velocity fields can be obtained. A comparison of velocity magnitude measured by the three approaches (i.e., 3D- LPTV, 2D- LPTV and LSPIV) is presented in Section 5.1.

4.4. Image correlation

The image positions of grid surface points in the first capture of the image sequence are used to perform the cross-correlation, which is employed to estimate the movement of surface patterns in the image sequences. In this study, zero mean normalized cross-correlation (ZNCC) is applied for both the multiple-camera-based approach and the single-camera approach. Considering two successive frames $F_1(\boldsymbol{u}_i)$ and $F_2(\boldsymbol{u}_j)$ with approximately the same features that are recorded at two-time instances, the ZNCC is expressed by equation (1),

$$C_{ZNCC} = \frac{\sum_{i,j=1}^{N} f_1(\boldsymbol{u}_i + \Delta\boldsymbol{u})\, f_2(\boldsymbol{u}_j)}{\sqrt{\sum_{i=1}^{N} f_1^2(\boldsymbol{u}_i + \Delta\boldsymbol{u}) \sum_{j=1}^{N} f_2^2(\boldsymbol{u}_j)}} \tag{1}$$

where $f = F - \langle F \rangle$ is the zeros-mean gray value, N is number of pixels in the subset, $\boldsymbol{u}_i$ and $\boldsymbol{u}_j$ denotes the coordinates that correspond to the reference and search images, and $\Delta\boldsymbol{u}$ is the correlation variable, that maps the reference subset to the search subset [40].

It is assumed that the motions of the features between the two frames are small, thus, local information can be utilized to estimate local motion. The procedure in image correlation is to pick out an IA from the reference image F_1 and search in a search area in the search image F_2 for the set $\Delta\boldsymbol{u}_{max}$ of the set $\Delta\boldsymbol{u}$ that maximizes the correlation value C_{ZNCC} in

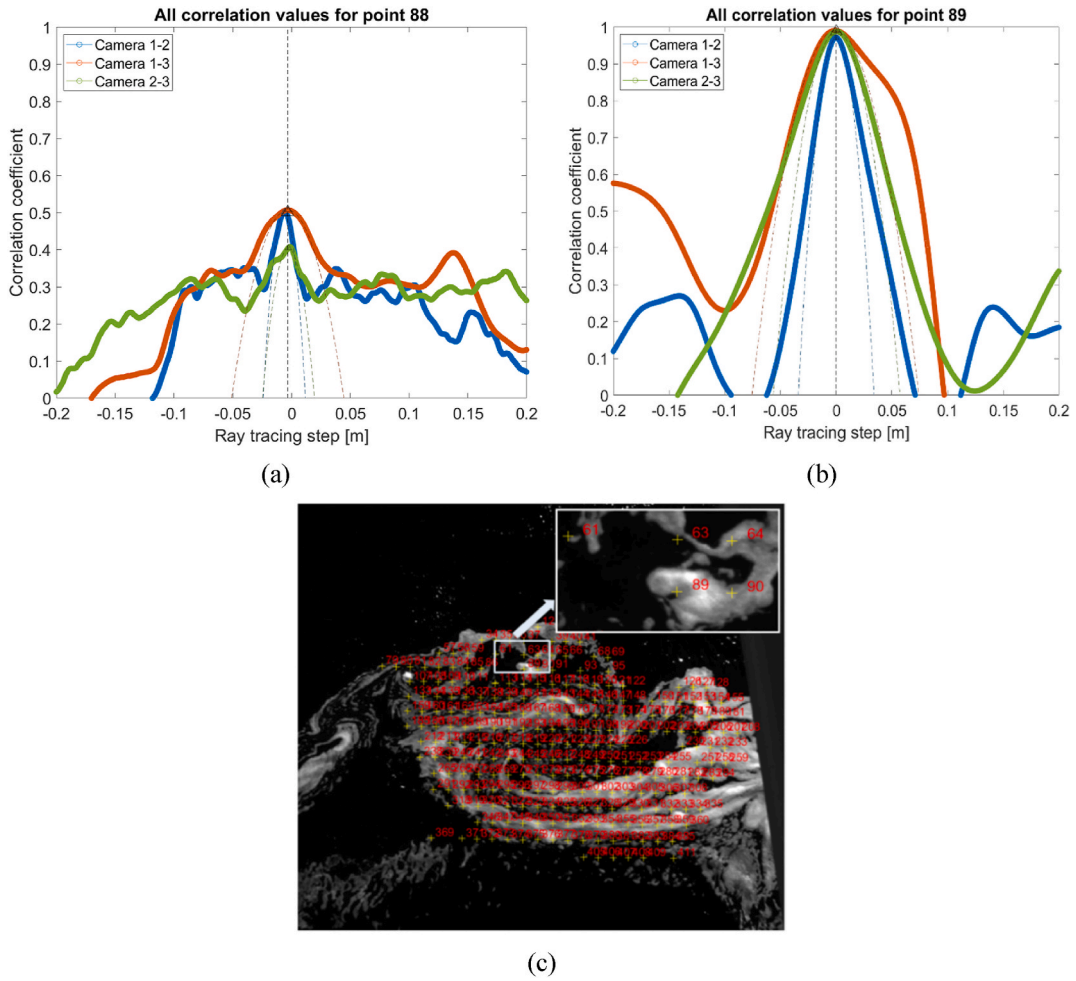

Fig. 4. Camera network correlation: (a) Invalid surface point; (b)Valid surface point; (c) Reprojection of valid 3D surface points onto image using camera network correlation.

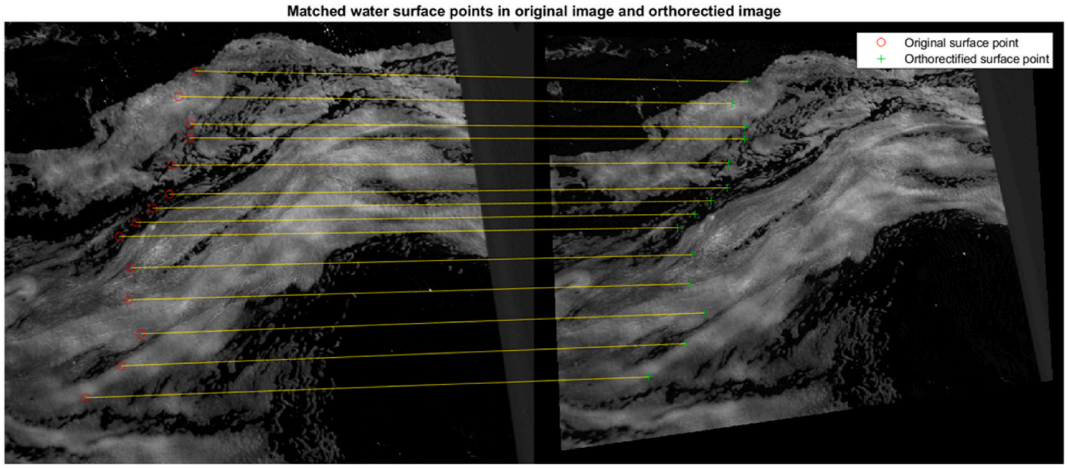

Fig. 5. An example of corresponding river surface points in the original image (left) and orthorectified image (right).

equation (1). The IA's local displacement vector is then estimated using the two translation components corresponding to the peak of the correlation map.

The interrogation is implemented as follows: The first pass begins by distributing a set number of points within the search area, which can be adjusted to a pixel level to reduce computation time. Its main objective is to roughly estimate the area within the search area where the peak is located (see Fig. 6b). Subsequently, in the second pass, cross-correlation is limited to a smaller search area surrounding the estimated peak region from the first pass. Operating at a sub-pixel level with an interval of 0.01 pixel, this step correlates the original IA in the search image with the reference image (see Fig. 6c). Finally, to avoid issues associated with the peak locking, a second order polynomial is utilized to fit the peak surface, considering the 6 points with the highest cross-correlation values

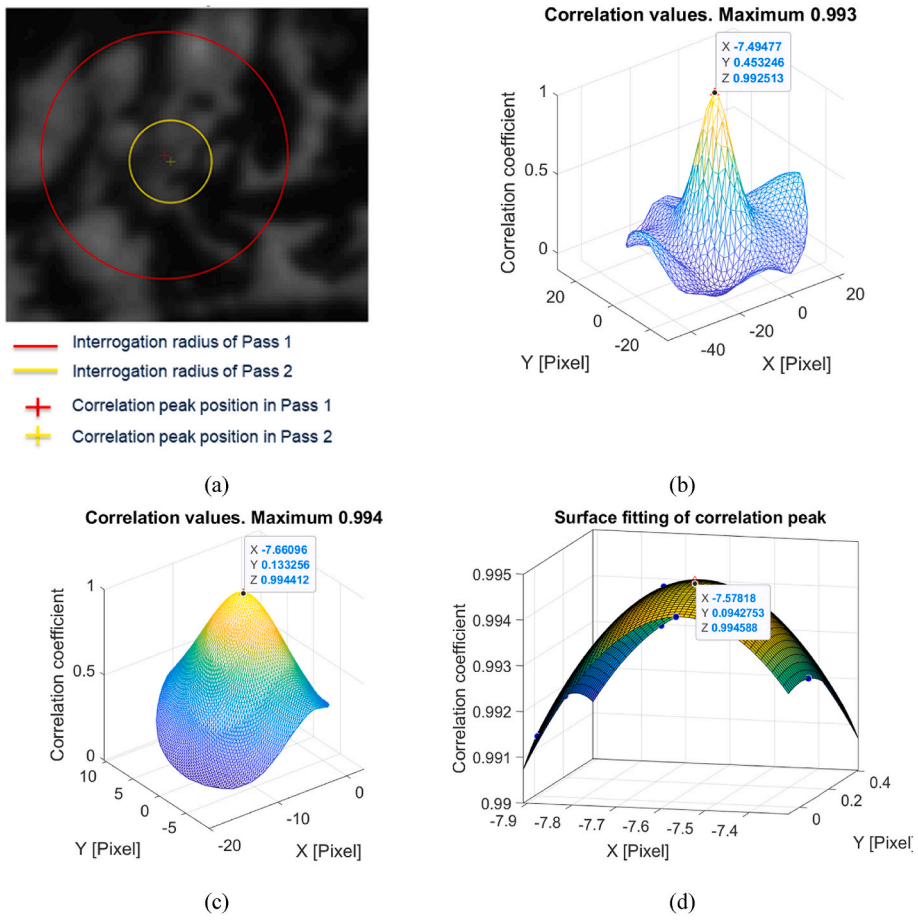

Fig. 6. An example of interrogation correlation procedure: (a) Two passes of cross correlation; (b) Correlation map of the first pass; (c) Correlation map of the second pass; (d) Surface fitting on correlation peak region.

within the peak region, allowing for the estimation of the most reliable peak on the correlation map (see Fig. 6d).

Image correlation is performed with orthorectified images to calculate 2D velocity distribution on the river surface. In 3D-LPTV, the defined surface points (as described in Section 4.1) are tracked in the image sequences of all cameras and their spatial coordinates are calculated by triangulation in the geometry of the camera network. Consequently, the surface pattern trajectories are reconstructed in 3D-LPTV analyses, as illustrated in Fig. 7. In 2D-LPTV and LSPIV, the valid surface points in the orthorectified images are transformed from their equivalents in the original images.

4.5. *Outlier filtering of velocity vector*

In image-based river velocimetry, outlier filtering is critical in order to improve the velocity estimation accuracy. Image cross-correlation-based filtering [33,41] and post-processing [42] are two common error-filtering strategies. Based on these principles, several methods for

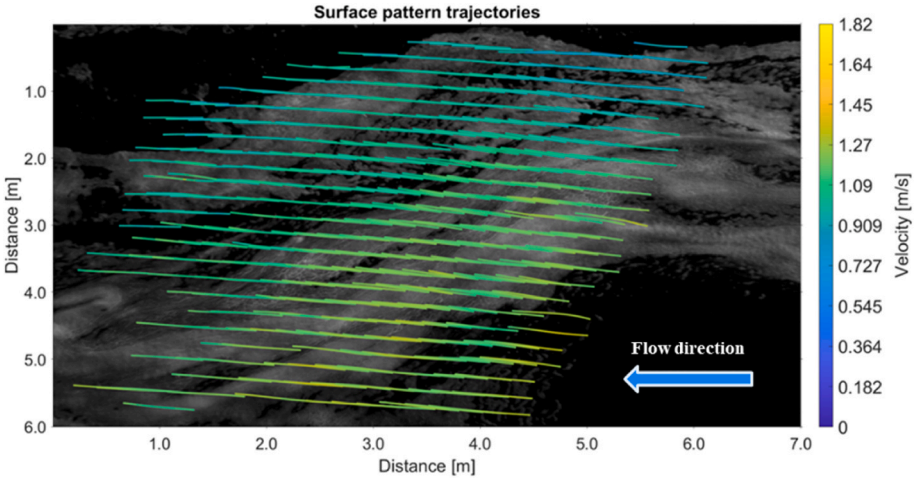

Fig. 7. An example of reconstructed surface pattern trajectories.

eliminating potentially inaccurate velocity vectors have been published. Tauro et al. [28] developed trajectory-based filtering for PTV using a priori knowledge of the flow direction. Recently Eltner et al. [43] proposed a track filtering criterion that includes a minimum proportion of frames in which features must be traceable, minimum and maximum distance limits, and flow direction. For the LSPIV application by Li et al. [33], the filtering procedures were based on the normalized correlation coefficient, the discarding of spurious vectors, and the global mean and standard deviation at each mesh point on the flow surface.

In this work, a filtering criterion that encompasses both strategies are applied in the image processing procedure as the three criteria presented below.

(1) The first criterion is used in the camera network correlation step to define grid points on the river surface (see section 4.1). A surface point is considered invalid if its median correlation coefficient is less than 0.9 or the difference in x-coordinate between the three correlation peaks is greater than a threshold value (see Fig. 4). The threshold value indicates the acceptability of the disparity of surface point coordinates determined by camera pairs in the imaging system. Here, this value is set to 1.0 cm.
(2) The second criterion is a correlation coefficient-based filter in image sequences, which is deployed in the correlation-based tracking process. A grid point is marked as invalid if its correlation coefficient between captures is less than 0.90.
(3) The third criterion detects outlier vectors in post-processing validation of the surface velocity field. The local mean velocity of each grid point is calculated from its surrounding grid points on a 3 × 3 mesh grid. The residual is defined as the difference between the measured velocity and the local median. A velocity vector is marked as an outlier if any of its velocity components have residuals that are two times greater or smaller than the median of its neighboring points.

5. Results and discussion

In Section 5.1, we present river surface velocities estimated by the three approaches, outlined in Fig. 3. The comparisons are conducted using five distinct datasets. Section 5.2 demonstrates the reconstruction of the river surface using 3D-LPTV. In Section 5.3, we investigate surface pattern characteristics such as intensity gradient and strength of cross-correlation peak to determine a relationship between characteristics of these river floating patterns and the precision of measured surface velocity. Discussion on these results is presented in Section 5.4.

5.1. Image velocimetry results from different approaches

This section assesses the performance of three different flow measurement techniques: 3D-LPTV, 2D-LPTV, and LSPIV. Each method is applied across five separate datasets, and their results are compared. The river surface features corresponding to the five datasets are highlighted in Fig. 10a. The outlier filtering criteria outlined in Section 4.4 are used in the image processing of all three techniques across the datasets. Velocity estimations for all three methods rely on matching river surface patterns. The comparison of the techniques is based on the average velocities and standard deviations (SDT) derived from the analyses. The 3D-LPTV technique estimates surface velocity using original images from all cameras, while 2D-LPTV and LSPIV employ orthorectified images. The results from the three approaches are summarized in Fig. 8.

5.2. River surface reconstruction

In the multiple-camera imaging system, when all corresponding river surface points are identified between image pairs, their spatial coordinates are determined through triangulation, following the methodology outlined in the 3D-LPTV approach. Fig. 9a shows the reconstruction of 3D points on the river surface and Fig. 9b shows a visualization of the observed water surface area achieved through interpolation of the measured 3D surface points. The river surface structure appears to have a height of approximately 5.0 cm. The third component of river surface coordinates provides information regarding their elevation in the defined coordinate system. By maintaining the same reference coordinate system when observing the river surface, variations in water level can be detected over time. The three-dimensional data of the water surface also allows for the detection of stage variations where applicable. Such information is crucial for discharge estimation, periodic analysis of reservoir conditions and potentially for flood warnings.

5.3. Characteristics of river surface patterns on uncertainty of measured velocity

Surface floating tracers observed on river surfaces exhibit a wide variety of appearances. The majority of these surface patterns observed during this measurement campaign were attributed to upstream spill flow. It's important to note that errors in river velocimetry arise from various factors within the procedure of the measurement from data acquisition (frame rate, stabilization of the camera, field conditions), pre-processing, main processing, and post-processing [35]. Here we exclusively focus on the impacts of surface flow patterns and the

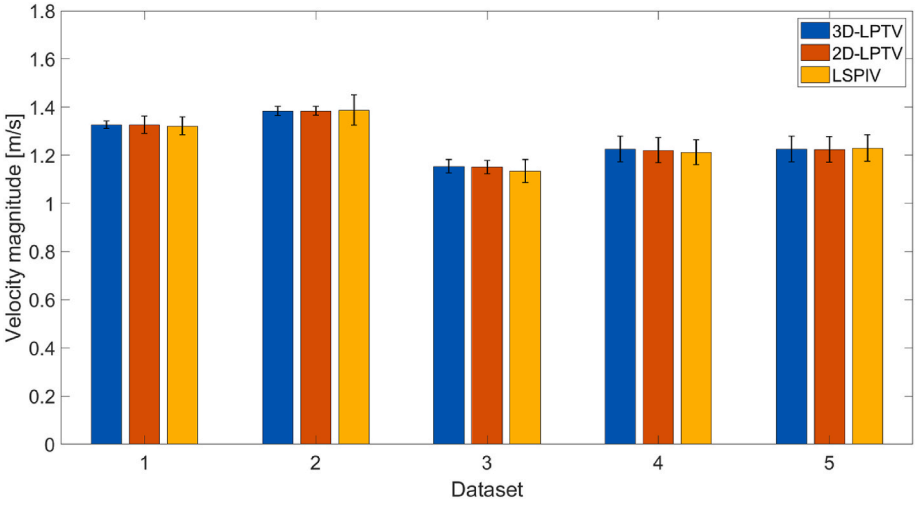

Fig. 8. Average measured velocity and standard deviation from five datasets.

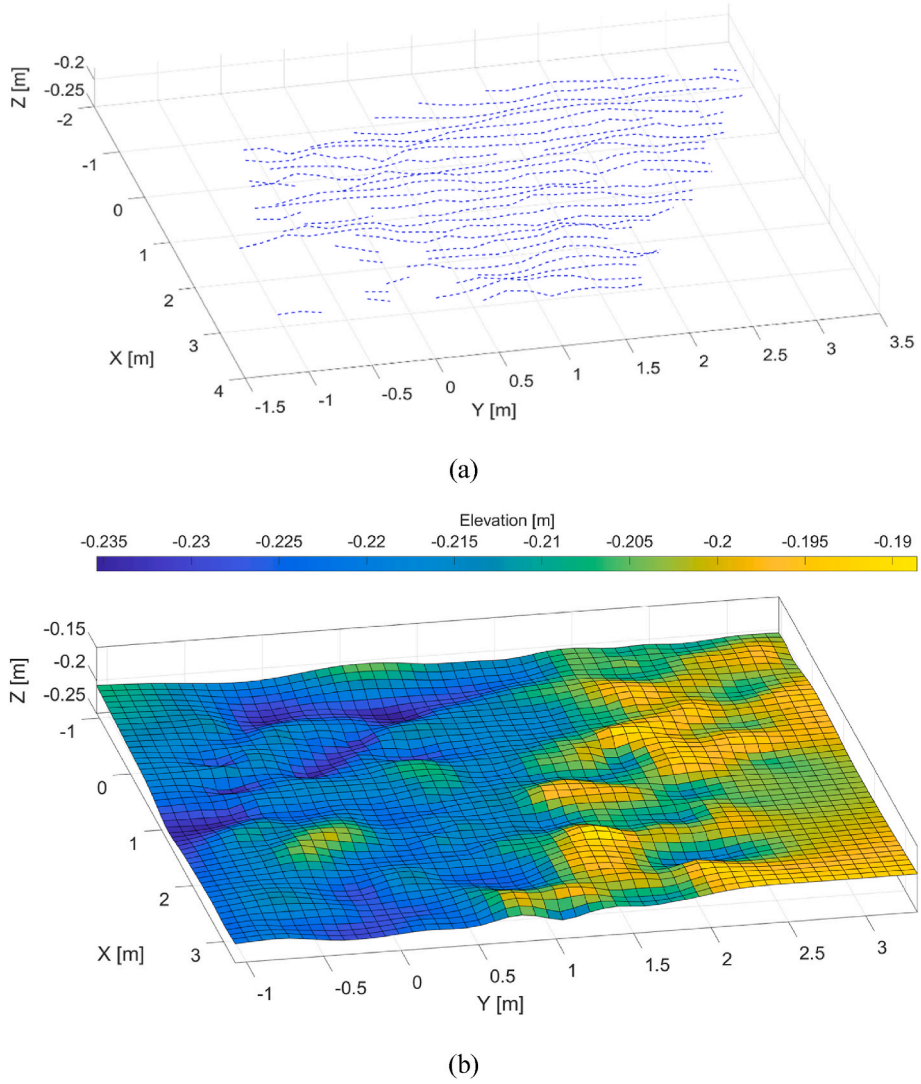

Fig. 9. An example of (a) 3D reconstructed river surface points, (b) Interpolation of river surface.

reliability of pattern-based image tracking on the precision of measured velocity. The purpose of this section is to investigate the properties of these surface floating patterns and establish a correlation between their imaging characteristics and the associated uncertainty in the measured velocity. The river surface features highlighted in Fig. 10a show the behaviors of floating tracers in the five reference datasets corresponding to the five surface patterns that will be utilized for analysis within this section.

It is well known that the size of the interrogation area in cross-correlation between consecutive frames influences the accuracy of the measured displacement. On one hand, the size of the IA should be sufficiently large enough to encompass a distinct intensity pattern and differentiate itself from other interrogation areas. On the other hand, employing a larger IA often results in increased errors when approximating underlying deformations.

Fig. 10b illustrates the standard deviation of the measurements from the five reference river surface patterns. The IA radii vary from 10 to 150 pixels with an increment of 10 pixels. It is evident that, across all river surface patterns, the standard deviations decrease as the interrogation areas increase. To ensure consistent analysis of image pattern characteristics, an interrogation radius of 50 pixels is selected for all five datasets. Therefore, the analyses in the following subsections are based on results obtained using the same interrogation area radius of 50 pixels for the velocity estimation.

5.3.1. *Image intensity gradient and uncertainty of measured velocity*

In nature, water surface patterns often exhibit inhomogeneity and varying density distributions. Fig. 10a illustrates the notable distinctions in feature size, distributions, and image contrast among these five surface floating patterns. To assess the relationship between pattern quality and the accuracy of measured displacement in correlation-based tracking methods, Pan et al. [44] introduced a parameter known as the intensity gradient, which is associated with the error in deformation measurement. Although Pan et al. [44] investigated the relationship between intensity gradient and accuracy of displacement measurement using Sum of Squared Differences (SSD) correlation criterion, Tong [45], Pan et al. [46], and Pan [47] prove that the zero-mean normalized sum of squared differences (ZNSSD) coefficient is directly related to the ZNCC and that ZNSSD and ZNCC criteria are equivalent. Thus, the interrogation area intensity gradient (IAIG) has an equivalent impact on the accuracy of displacement measurement when ZNCC is employed.

As shown in Figs. 2 and 10a, the natural tracers in the flow are distributed unevenly, leading to significant variations in the local parameters computed for different interrogation areas. In this study, we employ a local parameter referred to as the sum of square of interrogation area intensity gradient (SSIAIG) to assess the contrast of river surface pattern in each IA. The SSIAIG is computed for every valid surface point (see Section 4) as equation (2)

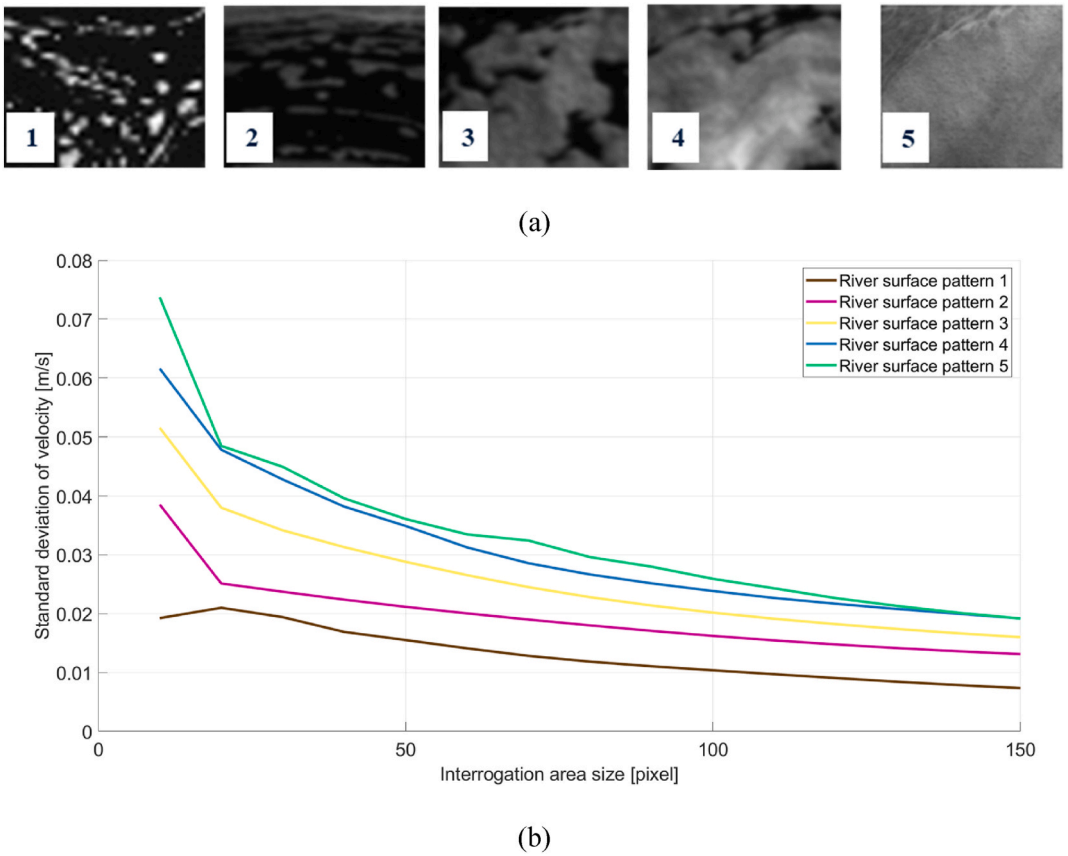

Fig. 10. (a) Cropped images from five river surface patterns; (b) Standard deviation of measured velocities for five datasets vs. the interrogation area sizes.

$$SSIAIG = \sum\sum |\nabla G(x,y)|^2 \tag{2}$$

where $|\nabla G(x,y)| = \sqrt{G_x^2 + G_y^2}$, with G_x and G_y are the local intensity gradient in interrogation area in x and y direction, respectively.

The SSIAIG value is calculated for the five datasets corresponding to five river surface patterns presented in Fig. 10a, using the same IA size. In Fig. 11a, the coefficients of variation are calculated as the averaged ratios of the standard deviation to the mean velocity for each dataset. The SSIAIG values represent the averages of SSIAIG values calculated from the river surface patterns within the five datasets. Fig. 11b illustrates the relationship between the measured velocity deviation and the SSIAIG for each data point.

5.3.2. *Peak to sidelobe ratio of cross-correlation map and standard deviation in measured velocity*

In both LSPIV and PIV techniques, the correlation coefficient obtained from cross-correlation is commonly employed as a criterion to evaluate the quality of image tracking. However, the lack of seeding particles or the presence of natural floating particles with poor visibility can significantly degrade the accuracy of the matching process. In such scenarios, the matching algorithm still attempts to identify the most similar result, which may result in an erroneous estimation of displacement. Notably, these inaccuracies cannot be detected by solely evaluating the correlation coefficient values.

The image-matching process is carried out using ZNCC, as described in Section 4.3. The PSR values are estimated to assess the quality of the cross-correlation-based tracking method. The PSR value is widely used in target tracking to evaluate the quality of tracking [48]. The calculation of PSR is provided by equation (3)

$$PSR = \frac{peak - mean}{standard\ deviation} \tag{3}$$

where *peak* stands for the maximum value of the cross-correlation of the interrogation window in the reference frame and searching frame, and *mean* and *standard deviation* are the mean and standard deviation of the sidelobe (see Fig. 12). In Fig. 13, an example of cross-correlation maps and their corresponding PSR values for two interrogation areas of two surface patterns are presented. According to the general behavior of the correlation function, a narrower and well-defined peak would lead to a more precise peak position and thus improve the accuracy of the deformation calculation [49].

The PSR values were calculated for each dataset, and the average PSR values are represented by orange circular dots in Fig. 14a. Correspondingly, the coefficient variations of the averaged velocities for the five datasets are denoted by blue circular dots. Note that these results were obtained using the 3D- LPTV method. Fig. 14b shows the distribution of measured velocity deviation and PSR of each data point.

5.4. *Discussion*

The averaged velocities and their STD estimated from the three approaches are shown in Fig. 8. The differences in results obtained by 3D-LPTV and LSPIV techniques range from 0.3% to 1.8% of the average velocity magnitude. For 3D- and 2D-LPTV methods, the standard deviations of velocity vary from 1.3% to 2.9%. However, for LSPIV, these values range from 2.8% to 4.4%, as shown in Fig. 8. The results show a high level of agreement in terms of averaged velocity across all three techniques. The difference in velocity magnitudes between 3D-LPTV and 2D-LPTV is found to be negligible, ranging from 0.01% to 0.4%. Therefore, the assumption of a planar river surface in this experiment is considered appropriate for the measurement. Notably, across all our datasets the uncertainties in measured velocities from the LSPIV technique are about two times larger than those from the other approaches. The discrepancy between the performance of LPTV-based and LSPIV

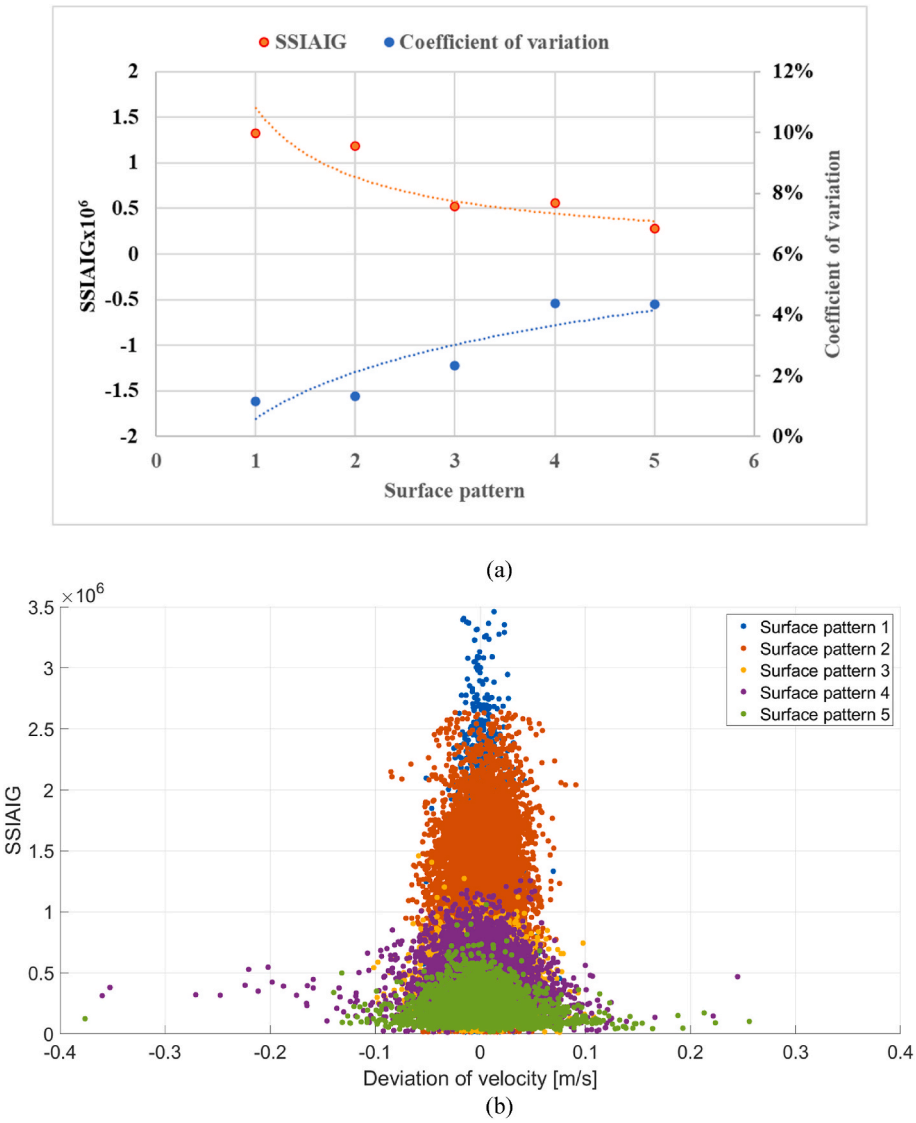

Fig. 11. (a) Coefficient variation of velocity and corresponding SSIAIG of five river surface patterns (1–5); (b) Distribution of measured velocity deviation and SSIAIG of each data point.

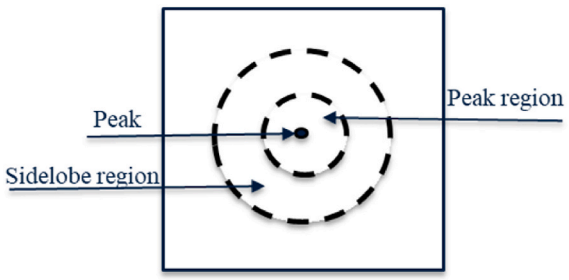

Fig. 12. The peak, peak region, and sidelobe region of cross-correlation.

techniques may be attributed to the presence of intermittent surface patterns within the field of view. Specifically, the LPTV-based tracking method relies on the displacement of recognizable surface patterns, while LSPIV measures the movement of water at every grid surface point regardless of the presence or absence of surface floating tracers. As a result, surface movement tracking is more prominent in the LPTV approach than in the PIV approach used for natural floating tracers in rivers. When using the PIV-based method for particle patterns that intermittently appear within the field of view, the lack of surface characteristics leads to a high level of uncertainty in the surface velocity. In summary, the results of the three approaches show that all three methods yield similar results in terms of averaged velocity. Nonetheless, the LPTV-based approach is considered more reliable because it produces lower standard deviation values. Datasets 4 and 5 show similar standard deviations in velocities across the three approaches (3D-LPTV, 2D-LPTV, LSPIV). Generally, these two datasets yield higher uncertainty in the results compared to the others. Fig. 10 highlights that patterns 4 and 5 resemble cloudy foam features, while patterns 1, 2, and 3 exhibit more discrete features. In the case of cloudy foam features, there is a higher level of measurement uncertainty across all approaches.

The choice of method for surface velocity measurements depends on the required output and the level of precision and accuracy needed. In natural streams, pattern-based tracking methods offer several advantages over particle tracking methods, including the ability to use natural floating patterns on river surfaces, relaxation of the requirement for tracer particles to have a well-defined shape and size, and applicability on a larger scale. However, natural tracer dispersion is often inhomogeneous, and surface patterns can vary significantly due to sunlight reflection, making outlier filtering critical for reliable results. In this paper, we use a filtering approach that incorporates both image-

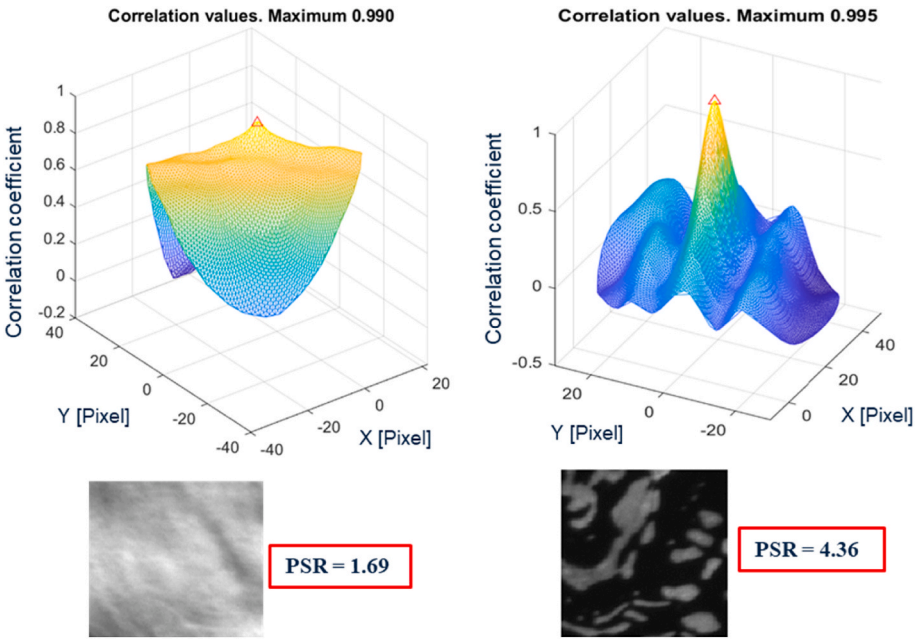

Fig. 13. Example of visualization of cross-correlation map corresponding to two interrogation areas of surface patterns and their PSR values.

matching and post-processing strategies. Specifically, we utilize a multiple-camera system that enables the detection of good regions on surface patterns for image tracking through the camera network correlation procedure. Another advantage of the multiple-camera system is the ability to reconstruct the river surface, allowing assessment of water level variation and water stage.

The ability to track identifiable surface particles or patterns is crucial for accurate image-based surface velocity measurements. While artificial tracer particles are commonly employed to enhance measurement reliability, challenges arise in large river conditions. In this context, natural floating tracers on the river surface offer valuable potential for river velocimetry using image analysis. This study explores the influence of surface-floating particles or tracers on image-based river velocimetry, emphasizing their crucial role in enhancing measurement accuracy and reliability. While controlling these tracers on the river surface can be challenging, selecting an appropriate IA size during image processing emerges as a crucial factor. The IA must encompass enough identifiable features to enable accurate tracking. Fig. 10 illustrates that to achieve the same precision in the measurement, the average IA size varies for each of the five reference river surface patterns. Specifically, for a STD of 0.02 m/s, the average IA size is as follows: 25 pixels for image pattern 1, 60 pixels for image pattern 2, 100 pixels for image pattern 3, and 140 pixels for image patterns 4 and 5. This indicates that utilizing a small subset can result in sufficient precision when measuring displacements in images with higher contrast. Therefore, the interrogation area size should be optimized according to the specific conditions of the surface floating tracer in order to improve the precision of the measurement.

Analyses on the intensity gradient of IA from the reference river surface patterns show that the standard deviations of measured velocities from river surface patterns 4 and 5 are larger than those obtained from river surface patterns 1 and 2 (see Fig. 11a). This discrepancy can be attributed to the progressive decrease in image contrast observed from pattern 1 to pattern 5. Fig. 11b shows the deviation in the measured velocity and SSIAIG for each point of all five river surface patterns. It is evident that the deviation in the measured velocity decreases as the SSIAIG increases. In addition to image contrast, the features in pattern 1 are smaller than those in the other patterns, and their distribution in the image is more uniform. These factors contribute to the higher intensity gradient calculated from river surface pattern 1 compared to the other patterns.

Fig. 14a illustrates that a negative correlation exists between the PSR values of the cross-correlation process and the measurement uncertainty. River surface pattern 1, which has the highest value of PSR exhibited the smallest velocity variation, while dataset 5, which has the lowest PSR value, shows the largest coefficient of variation. This result highlights the inverse relationship between decreasing PSR values and increasing coefficient variation in measured velocity. A higher PSR typically indicates a stronger correlation peak relative to sidelobes, implying more accurate measurements. Furthermore, among the five patterns, patterns 4 and 5 are particularly susceptible to variations in brightness and contrast caused by sunlight. As these variations are unrelated to flow movement, they contribute to the overall uncertainty of the measurement. The strength of the cross-correlation map in image tracking emerges as a valuable parameter for filtering, contributing to the overall reliability of measured velocity. This parameter holds the potential to improve displacement determination accuracy, thereby improving the quality of the measured velocity.

Both image intensity gradient and PSR serve as indicators of the surface floating pattern characteristics. The analysis demonstrates the important role these characteristics play in improving the precision of the velocity measurements. The ZNCC algorithm used for cross-correlation between consecutive images in the same sequence (as presented in Section 4.1), is also the underlying process in camera-to-camera correlations within the camera network, in which it measures the similarity between homologous sub-images in camera pairs. Surface patterns that are more susceptible to sunlight reflection may be imaged slightly differently in different cameras in the same camera network. This issue lowers the PSR of the cross-correlation process and consequently increases the uncertainty in determining homologous surface points, negatively impacting the measurement accuracy. Through our analysis, we identify that patterns 4 and 5 are particularly vulnerable to this phenomenon. Consequently, the uncertainties in velocity measurements for patterns 4 and 5 are larger than those of the other river surface patterns. The analysis of SSIAIG of image patterns and PSR of cross-correlation in image tracking demonstrates that patterns with small size, high contrast, evenly redistributed, and higher density of particles are better for measurement reliability. Both SSIAIG and PSR serve as metrics for assessing the suitability of natural surface floater in image-based river velocimetry. Optimizing IA size based on SSIAIG and employing PSR as a filtering criterion could significantly enhance the

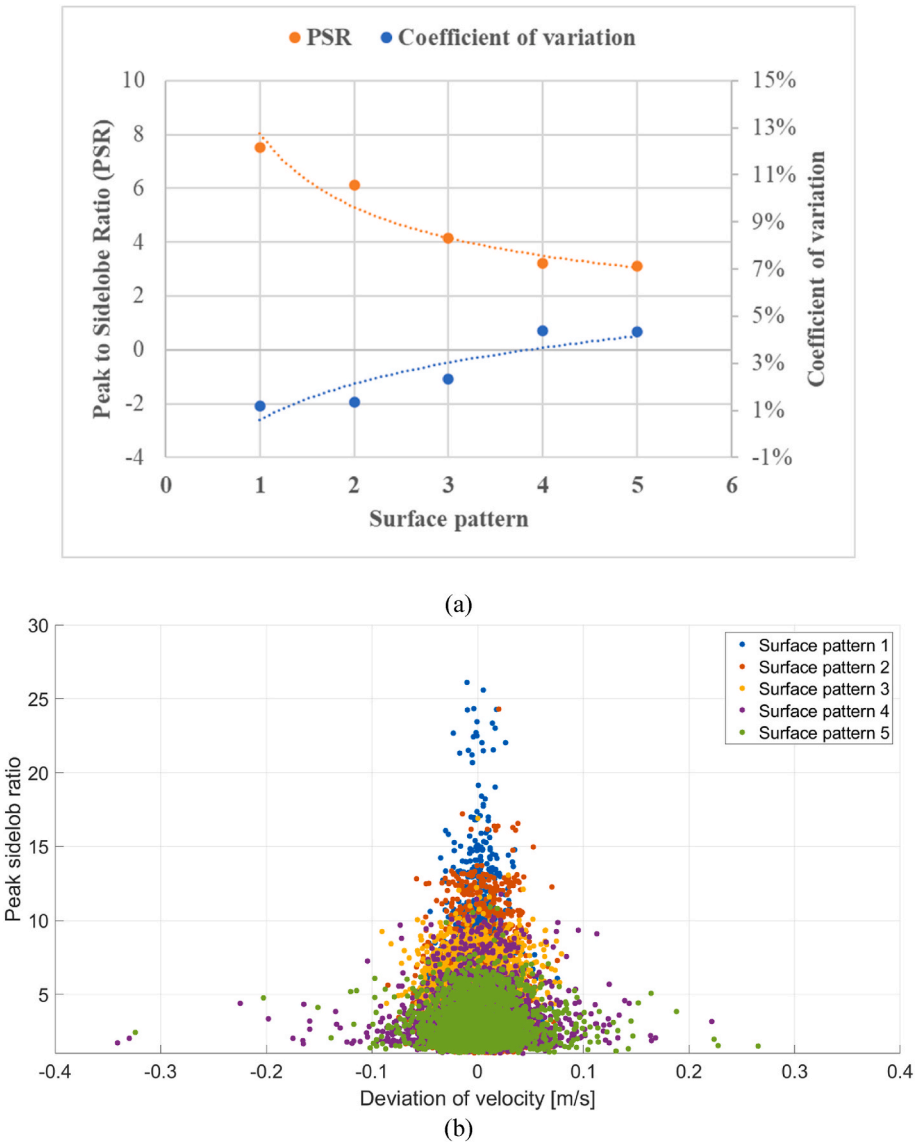

Fig. 14. (a) Coefficient variation of velocity and corresponding PSR of five river surface patterns (1–5); (b) Distribution of measured velocity deviation and PSR of each data point.

reliability of measurements in river velocimetry.

Accurate image-based velocity measurements depend not only on the choice of algorithm and its parameters but also on several other factors, such as the measurement setup, camera calibration, and image processing method. Camera calibration is a crucial step to minimize image distortion, which can lead to significant errors in velocity measurements. Detert [50] reported that the accuracy of image velocimetry is greatly improved with a careful calibration process. In the presence of wind, image velocimetry should not be used for low flow conditions due to the generation of small waves, such as capillary waves or ripples, by surface wind. These waves travel at their own speed and direction and can result in measurement errors.

6. Conclusions

In this study, we examine the performance of image-based velocity measurements in natural flow conditions using a pattern-based tracking technique. By utilizing a multiple-camera system, we employ a camera network correlation procedure that can effectively identify and track intermittent surface patterns, allowing for the selection of only the most reliable regions for tracking.

We applied pattern-based tracking to the same datasets to validate the performance of the three approaches: 3D-LPTV, 2D-LPTV, and LSPIV. All approaches produce good agreement between the three in terms of averaged velocity. However, the LSPIV shows larger standard deviations of velocity, ranging from 2.8% to 4.4%, compared to 1.3%–2.9% from the 3D and 2D- LPTV methods, respectively. The differences in velocity magnitudes between 3D and 2D are within the range of 0.1%–0.4%. However, one advantage of using the same reference coordinate system for observations is the ability to reconstruct the river surface and detect variations in water level over time.

An analysis of the characteristics of river floating patterns was performed to understand their effects on measurement accuracy. The river surface patterns associated with small feature sizes and even distribution give higher SSIAIG values and subsequently provide higher precision of measured velocities. The patterns with higher PSR values correspond to higher precision in measured velocities indicating that the quality of cross-correlation, as measured by PSR, valuable parameter for filtering, contributing to the overall reliability of measurement results. Both SSIAIG and PSR could be used for evaluating the suitability of natural surface patterns in image-based river velocimetry. River flow measurements are greatly beneficial by the image-based technique.

Understanding the primary factors that impact the reliability of the measurement allows individuals to make better decisions, from choosing an appropriate measurement approach to data acquisition and image analysis.

Funding

This research was funded by Svenskt Vattenkraftcentrum, SVC ("The Swedish Hydropower Center").

CRediT authorship contribution statement

Hang Trieu: Writing – review & editing, Writing – original draft, Visualization, Validation, Software, Methodology, Formal analysis, Data curation, Conceptualization. **Per Bergström:** Writing – review & editing, Validation, Supervision, Software, Methodology, Data curation, Conceptualization. **Mikael Sjödahl:** Writing – review & editing, Validation, Supervision, Methodology. **J.Gunnar I. Hellström:** Writing – review & editing, Validation, Supervision, Project administration. **Patrik Andreasson:** Writing – review & editing, Validation, Resources, Project administration. **Henrik Lycksam:** Writing – review & editing, Data curation.

Declaration of competing interest

The authors declare that they have no known competing financial interests or personal relationships that could have appeared to influence the work reported in this paper.

Data availability

Data will be made available on request.

Acknowledgment

The research presented has been carried out as a part of "Swedish Hydropower Centre/SVC". SVC has been established by the Swedish Energy Agency, Energiforsk and Svenska Kraftnät together with Luleå University of Technology, Chalmers University of Technology, The Royal Institute of Technology and Uppsala University.

The authors would also like to thank Mr Kristian Söderholm from Viospatia AB, Sweden for his technical support related to camera synchronization.

References

[1] U. Förstner, Sediment dynamics and pollutant mobility in rivers: an interdisciplinary approach, Lakes Reservoirs Res. Manag. 9 (1) (2004) 25–40.
[2] G. Govers, Relationship between discharge, velocity and flow area for rills eroding loose, non-layered materials, Earth Surf. Process. Landforms 17 (5) (1992) 515–528.
[3] J. Nestler, R. Goodwin, D. Smith, J. Anderson, S. Li, Optimum fish passage and guidance designs are based in the hydrogeomorphology of natural rivers, River Res. Appl. 24 (2) (2008) 148–168.
[4] A.T. Piper, C. Manes, F. Siniscalchi, A. Marion, R.M. Wright, P.S. Kemp, Response of seaward-migrating European eel (Anguilla anguilla) to manipulated flow fields, Proc. Biol. Sci. 282 (1811) (2015) 20151098.
[5] P. Dobriyal, R. Badola, C. Tuboi, S.A. Hussain, A review of methods for monitoring streamflow for sustainable water resource management, Appl. Water Sci. 7 (6) (2017) 2617–2628.
[6] R.W. Healy, T.C. Winter, J.W. LaBaugh, O.L. Franke, Water Budgets: Foundations for Effective Water-Resources and Environmental Management, US Geological Survey Reston, Virginia, 2007.
[7] M. Muste, T. Vermeyen, R. Hotchkiss, K. Oberg, Acoustic Velocimetry for Riverine Environments, American Society of Civil Engineers, 2007, pp. 1297–1298.
[8] I. Fujita, M. Muste, A. Kruger, Large-scale particle image velocimetry for flow analysis in hydraulic engineering applications, J. Hydraul. Res. 36 (3) (1998) 397–414.
[9] J. Le Coz, A. Hauet, G. Pierrefeu, G. Dramais, B. Camenen, Performance of image-based velocimetry (LSPIV) applied to flash-flood discharge measurements in Mediterranean rivers, J. Hydrol. 394 (1–2) (2010) 42–52.
[10] R. Tsubaki, I. Fujita, S. Tsutsumi, Measurement of the flood discharge of a small-sized river using an existing digital video recording system, J. Hydro-environ. Res. 5 (4) (2011) 313–321.
[11] Swedish Energy Agency, Energy in Sweden 2022 an Overview, Eskilstuna, Sweden, 2020. www.energimyndigheten.se.
[12] R. Kostaschuk, J. Best, P. Villard, J. Peakall, M. Franklin, Measuring flow velocity and sediment transport with an acoustic Doppler current profiler, Geomorphology 68 (1–2) (2005) 25–37.
[13] D.S. Mueller, C.R. Wagner, M.S. Rehmel, K.A. Oberg, F. Rainville, Measuring Discharge with Acoustic Doppler Current Profilers from a Moving Boat, US Department of the Interior, US Geological Survey Reston, Virginia (EUA), 2009.
[14] J. Costa, R. Cheng, F. Haeni, N. Melcher, K. Spicer, E. Hayes, W. Plant, K. Hayes, C. Teague, D. Barrick, Use of radars to monitor stream discharge by noncontact methods, Water Resour. Res. 42 (7) (2006).
[15] J.A. Puleo, T.E. McKenna, K.T. Holland, J. Calantoni, Quantifying riverine surface currents from time sequences of thermal infrared imagery, Water Resour. Res. 48 (1) (2012).
[16] R.J. Adrian, Particle-imaging techniques for experimental fluid mechanics, Annu. Rev. Fluid Mech. 23 (1) (1991) 261–304.
[17] R.J. Adrian, Twenty years of particle image velocimetry, Exp. Fluid 39 (2) (2005) 159–169.
[18] S. Baek, S. Lee, A new two-frame particle tracking algorithm using match probability, Exp. Fluid 22 (1) (1996) 23–32.
[19] I. Fujita, H. Watanabe, R. Tsubaki, Development of a non-intrusive and efficient flow monitoring technique: the space-time image velocimetry (STIV), Int. J. River Basin Manag. 5 (2) (2007) 105–114.
[20] B.D. Lucas, T. Kanade, An Iterative Image Registration Technique with an Application to Stereo Vision, Vancouver, 1981.
[21] M.T. Perks, A.J. Russell, A.R. Large, Advances in flash flood monitoring using unmanned aerial vehicles (UAVs), Hydrol. Earth Syst. Sci. 20 (10) (2016) 4005–4015.
[22] S. Dal Sasso, A. Pizarro, C. Samela, L. Mita, S. Manfreda, Exploring the optimal experimental setup for surface flow velocity measurements using PTV, Environ. Monit. Assess. 190 (8) (2018) 1–14.
[23] S.F. Dal Sasso, A. Pizarro, S. Manfreda, Metrics for the quantification of seeding characteristics to enhance image velocimetry performance in rivers, Rem. Sens. 12 (11) (2020) 1789.
[24] S.F. Dal Sasso, A. Pizarro, S. Pearce, I. Maddock, S. Manfreda, Increasing LSPIV performances by exploiting the seeding distribution index at different spatial scales, J. Hydrol. 598 (2021) 126438.
[25] A. Pizarro, S.F. Dal Sasso, S. Manfreda, Refining image-velocimetry performances for streamflow monitoring: seeding metrics to errors minimization, Hydrol. Process. 34 (25) (2020) 5167–5175.
[26] D. Strelnikova, G. Paulus, S. Käfer, K.-H. Anders, P. Mayr, H. Mader, U. Scherling, R. Schneeberger, Drone-based optical measurements of heterogeneous surface velocity fields around fish passages at hydropower dams, Rem. Sens. 12 (3) (2020) 384.
[27] F. Tauro, A. Petroselli, M. Porfiri, L. Giandomenico, G. Bernardi, F. Mele, D. Spina, S. Grimaldi, A novel permanent gauge-cam station for surface-flow observations on the Tiber River, Geosci. Instr., Meth. Data Syst. 5 (1) (2016) 241–251.
[28] F. Tauro, R. Piscopia, S. Grimaldi, Streamflow observations from cameras: large-scale particle image velocimetry or particle tracking velocimetry? Water Resour. Res. 53 (12) (2017) 10374–10394.
[29] G. Dramais, J. Le Coz, B. Camenen, A. Hauet, Advantages of a mobile LSPIV method for measuring flood discharges and improving stage–discharge curves, J. Hydro-Environ. Res. 5 (4) (2011) 301–312.
[30] F. Tauro, R. Piscopia, S. Grimaldi, PTV-Stream: a simplified particle tracking velocimetry framework for stream surface flow monitoring, Catena 172 (2019) 378–386.
[31] M. Detert, V. Weitbrecht, A low-cost airborne velocimetry system: proof of concept, J. Hydraul. Res. 53 (4) (2015) 532–539.
[32] A. Patalano, C.M. García, A. Rodríguez, Rectification of image velocity results (RIVeR): a simple and user-friendly toolbox for large scale water surface particle image velocimetry (PIV) and particle tracking velocimetry (PTV), Comput. Geosci. 109 (2017) 323–330.
[33] W. Li, Q. Liao, Q. Ran, Stereo-imaging LSPIV (SI-LSPIV) for 3D water surface reconstruction and discharge measurement in mountain river flows, J. Hydrol. 578 (2019) 124099.
[34] H. Trieu, P. Bergström, M. Sjödahl, J.G.I. Hellström, P. Andreasson, H. Lycksam, Photogrammetry for free surface flow velocity measurement: from laboratory to field measurements, Water 13 (12) (2021) 1675.
[35] M.J. Jolley, A.J. Russell, P.F. Quinn, M.T. Perks, Considerations when applying large-scale PIV and PTV for determining river flow velocity, Front. Water. 3 (2021) 1–21.
[36] S. Pearce, R. Ljubičić, S. Peña-Haro, M. Perks, F. Tauro, A. Pizarro, S.F. Dal Sasso, D. Strelnikova, S. Grimaldi, I. Maddock, An evaluation of image velocimetry techniques under low flow conditions and high seeding densities using unmanned aerial systems, Rem. Sens. 12 (2) (2020) 232.
[37] F. Tauro, A. Petroselli, S. Grimaldi, Optical sensing for stream flow observations: a review, J. Agric. Eng. 49 (4) (2018) 199–206.
[38] Q.W. Lewis, E.M. Lindroth, B.L. Rhoads, Integrating unmanned aerial systems and LSPIV for rapid, cost-effective stream gauging, J. Hydrol. 560 (2018) 230–246.
[39] P.I. Corke, O. Khatib, Robotics, Vision and Control: Fundamental Algorithms in MATLAB, Springer, 2011.
[40] M. Sjödahl, Gradient correlation functions in digital image correlation, Appl. Sci. 9 (10) (2019) 2127.

[41] L. Li, H. Yan, A robust filtering algorithm based on the estimation of tracer visibility and stability for large scale particle image velocimetry, Flow Meas. Instrum. 87 (2022) 102204.
[42] T. Jin, Q. Liao, Application of large scale PIV in river surface turbulence measurements and water depth estimation, Flow Meas. Instrum. 67 (2019) 142–152.
[43] A. Eltner, H. Sardemann, J. Grundmann, Flow velocity and discharge measurement in rivers using terrestrial and unmanned-aerial-vehicle imagery, Hydrol. Earth Syst. Sci. 24 (3) (2020) 1429–1445.
[44] B. Pan, H. Xie, Z. Wang, K. Qian, Z. Wang, Study on subset size selection in digital image correlation for speckle patterns, Opt Express 16 (10) (2008) 7037–7048.
[45] W. Tong, An evaluation of digital image correlation criteria for strain mapping applications, Strain 41 (4) (2005) 167–175.
[46] B. Pan, H. Xie, Z. Guo, T. Hua, Full-field strain measurement using a two-dimensional Savitzky-Golay digital differentiator in digital image correlation, Opt. Eng. 46 (3) (2007) 33601.
[47] B. Pan, Recent progress in digital image correlation, Exp. Mech. 51 (2011) 1223–1235.
[48] D.S. Bolme, J.R. Beveridge, B.A. Draper, Y.M. Lui, Visual object tracking using adaptive correlation filters, in: Proc., IEEE Computer Society Conference on Computer Vision and Pattern Recognition, IEEE, 2010, pp. 2544–2550.
[49] M. Sjödahl, Accuracy in electronic speckle photography, Appl. Opt. 36 (13) (1997) 2875–2885.
[50] M. Detert, How to avoid and correct biased riverine surface image velocimetry, Water Resour. Res. 57 (2) (2021) e2020WR027833.